Dual Mode SWIPT: Waveform Design and Transceiver Architecture with Adaptive Mode Switching Policy

Jong Jin Park, Jong Ho Moon, Kang-Yoon Lee, and Dong In Kim
College of Information and Communication Engineering
Sungkyunkwan University (SKKU), Korea
Email: {pjj0805, moonjh525, klee, dongin}@skku.edu

***Abstract*—In this paper, we propose a *dual mode* simultaneous wireless information and power transfer (SWIPT) system in which a sensor node monitors the received power and adaptively controls the communication mode. To this end, we design two types of single and multi-tone waveforms and propose a new transceiver architecture that realizes adaptive power management and information decoding (adaptive PM-&-ID) module. On top of this, we implement adaptive PM-&-ID policy algorithm which reflects non-linear energy harvesting (EH) model for both single and multi-tone waveforms. Our newly designed SWIPT can be applied to Internet-of-Things (IoT) network with RF EH capability for self-powering, leading to *battery-free* network. Numerical results show that significant performance gain can be achieved by the proposed dual mode SWIPT over the existing SWIPT design.**

***Index Terms*—Dual mode SWIPT, non-linear energy harvesting, adaptive power management, mode switching.**

I. Introduction

With the growing interest in Internet-of-Things (IoT), battery lifetime becomes a critical issue for operating IoT network perpetually. Low-power IoT devices need to be self-powered for energy neutral operation. Self-powered devices, charged from ambient renewable resources instead of battery replacement, can be deployed to self-sustain the IoT network. One of promising solutions is simultaneous wireless information and power transfer (SWIPT) [1] - [3], a technique that transfers both information and power in the air using a radio frequency (RF) signal. The received signal is used for harvesting energy as well as decoding information. The SWIPT using a single tone with various receiver types was addressed in [4].

Recently, it was shown that the RF-to-DC conversion efficiency of the rectifier in energy harvesting (EH) circuit typically increases with input power, but decreases at high input power because of the diode saturation effect [5]. In [6] and [7], using multi-sine (tone) waveforms can boost up the efficiency of wireless power transfer (WPT) due to the non-linear rectification process. Based on this non-linear model, more mathematically accurate multi-sine WPT efficiency and waveform optimization was suggested in [8]. However, these models focused only on the saturation effect when using single tone EH [5], or non-linear small signal model (not for the saturation effect) of the diode when using multi-tone EH [7], [8]. Non-linear energy harvesting model of the practical EH circuit must consider both the non-linear diode characteristics at low input power (i.e., small signal model) and the saturation effect at high input power regardless of single or multi-tone waveform. To the best of our knowledge, this issue has not been addressed in the literature.

Further, a single tone amplitude/phase modulation may not be used with multi-sine waveforms. To tackle this difficulty, we have proposed the peak-to-average power ratio (PAPR) based SWIPT [9], a technique that uses multi-sine waveforms and their distinct levels of PAPR to convey information. The PAPR based SWIPT achieves higher efficiency of WPT which increases the operational range, with less energy and low complexity for information decoding. But it suffers lower rate than that of the single tone based SWIPT. Hence, we should optimize the rate-energy tradeoff with the operational range. In high-end human-to-human (H2H) communications, we employ adaptive modulation and coding scheme (MCS) depending on channel quality. In the same spirit, in low-end machine-to-machine (M2M) communications, self-powered devices via SWIPT may control the communication mode depending on the received power for energy neutral operation. Adapting the communication mode according to the received power is crucial for self-powered devices in IoT applications. This has also motivated our work.

In this paper, we propose a dual mode SWIPT through optimum waveform design and new transceiver architecture. Here, the dual mode refers to two types of communication modes which are single tone and multi-tone (PAPR) based SWIPTs. The proposed transceiver monitors the received power and controls the communication mode via adaptive power management and information decoding (adaptive PM-&-ID) policy, considering the proposed non-linear EH model for energy neutral power management. It meets the *energy causality* for perpetual operation of self-powered devices.

II. System Model

We consider frequency flat (FF) fading channel for point-to-point SWIPT systems with one transmitter and one receiver, each equipped with a single antenna, while our design can be applied for the multi-antenna case. We assume that the receiver sends a short pilot signal to the transmitter before each frame transmission to estimate the channel gains (i.e., CSIT

978-1-5386-6355-4/18/$31.00 ©2018 IEEE

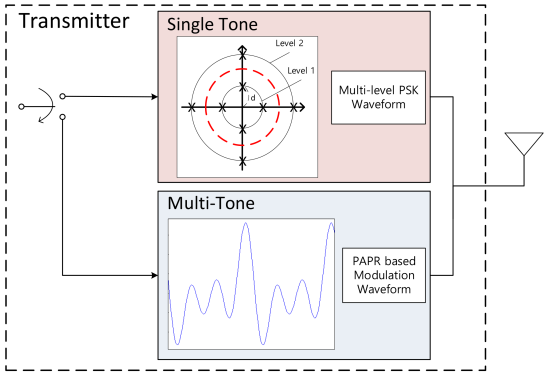

(a) Dual mode signaling

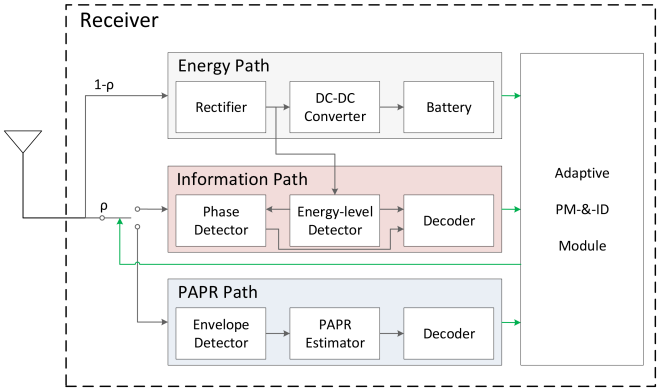

(b) Integrated receiver

Fig. 1. A new transceiver architecture for dual mode SWIPT.

is assumed). Let h denote the complex channel gain of the fading channel over which the transmitter sends a Gaussian-distributed symbol with average power P_T.

A. Non-linear Energy Harvesting Model

As shown in Fig. 1(b), the EH circuit consists of three components, such as a diode rectifier, DC-DC converter, and a battery. Because of the diode non-linear behavior (diode turn-on/breakdown voltage, non-linear diode equation, and saturation effect reported in [5]–[7]), the harvested power P_{EH} cannot be simply expressed by conventional linear model. To address the diode saturation issue, the non-linear EH model based on logistic function was suggested in [5], with which the fitted harvested power P_{NL} is given by

$$P_{NL} = \frac{P_{sat}(1 - e^{-aP_R})}{1 + e^{-a(P_R - b)}} \tag{1}$$

where P_{sat} is the maximum harvested power when the EH circuit is saturated, and P_R the received signal power. Here, a and b are the constants related to the EH circuit specification. Given the EH circuit, we can obtain P_{sat}, a and b using a curve fitting tool. However, the non-linear model of (1) may be inaccurate when the range of the received power is large.

Fig. 2(a) shows the logistic curve fitted results over wide range of the received power (P_R is -30dBm to 30dBm) using multi-tone $Q = 1, 2, 4$, where Q is the number of multi-sine waveforms. We can observe a gap of the harvested

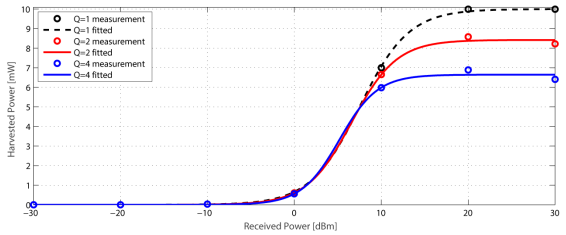

(a)

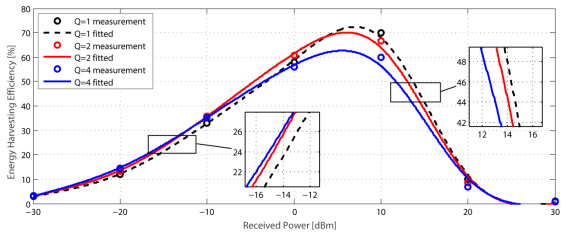

(b)

Fig. 2. Curve fitting of the non-linear energy harvesting model. Measurement data was obtained by using PSpice simulation.

power at high received power, but a negligible gap at low received power. In the latter, small curve fitting error can cause significant harvested power difference. Thus, this model is not appropriate to precisely predict the results obtained from non-linear rectification process of multi-sine small signal [7]. To resolve this problem, we convert the harvested power versus received power relationship to the EH efficiency versus received power one, defined by $P_{eff} = P_{EH}/P_R$. Due to this conversion, the non-linear model based on logistic function cannot be used to fit into the EH efficiency which is evaluated from the measurement data. Instead, we introduce a smoothing spline curve fitting method which is non-parametric. Given the data set of (x_i, y_i), where $y_i = \Psi_{EH}(x_i)$ for $i = 1, \ldots, k$, the cubic smoothing spline estimate $\hat{\Psi}_{EH}$ of the EH efficiency function $P_{eff} = \Psi_{EH}(P_R)$ is defined as the minimizer of the following optimization problem

$$\text{(P0)}: \min_{\hat{\Psi}_{EH}} \sum_{i=1}^{k} \left\{ y_i - \hat{\Psi}_{EH}(x_i) \right\}^2 + \lambda \int \hat{\Psi}''_{EH}(x)^2 \, dx$$

where λ represents a smoothing parameter obtained from the curve fitting tool. In Fig. 2(b), the EH efficiency obtained by using the smoothing spline curve fitting method is plotted over wide input range. It can be observed that multi-tone shows better efficiency in low received power region, which matches the results from small signal model in [7]. However, due to the saturation effect, single tone shows better EH efficiency when the received power is high. In other words, multi-sine waveforms have large voltage swing due to large PAPR, which leads to more clipping at high power. Following this observation, we may switch the communication mode adaptively to achieve the maximum harvested power. For this, we define the received power threshold P_{th} for mode switching, which depends only on the circuit specification.

B. Waveform Design and Transmitter Architecture

For the dual mode SWIPT, an integrated transmitter generates two types of single and multi-tone waveforms, as shown in Fig. 1(a). The transmitter selects a waveform according to the proposed adaptive PM-&-ID policy, which depends on the received power at the receiver.

Single tone/multi-level PSK. The single tone waveform is optimized for high data rate relative to the multi-tone one. We consider a single tone signaling of multi-energy level with phase-shift keying (PSK), which is expressed as

$$s_s(t) = \text{Re}\left\{A\exp(j2\pi f_c t + j\theta)\right\} \tag{2}$$

where $A \in \{\alpha, 2\alpha, ..., N_e\alpha\}$ and $\theta \in \{\frac{2\pi}{N_p}, 2\frac{2\pi}{N_p}, ..., 2\pi\}$ are the amplitude and phase of the modulated symbol, and f_c is the center frequency of the signal. N_e denotes the number of energy levels, and N_p the number of signal (phase) points per level. The unit amplitude α can be evaluated from the average signal power relationship as

$$P_T = \frac{N_p \sum_{l=1}^{N_e} (ld)^2}{M} \tag{3}$$

where $d = \alpha/\sqrt{2}$ is the constellation unit distance as indicated in Fig. 1(a), and M is the modulation index expressed as $M = N_e N_p$. The energy-level/phase information is decoded jointly at the receiver. The former maps to distinct energy levels (e.g., inner/outer circles in Fig. 1(a)), while the latter signal (phase) constellation points at a given energy level.

Multi-tone/PAPR modulation. As the distance from access point (AP) is farther, the transmit power should be increased to compensate for the severe propagation loss. We may enhance the efficiency of WPT by using multi-sine waveforms, which effectively increases the operational range, thanks to the non-linear rectification process. Furthermore, the PAPR based information transmission facilitates low-energy decoding via simple PAPR measurements [9]. The PAPR modulated signal which uses N subset tones from Q available tones (i.e., $N \in \{1, ..., Q\}$) is expressed as

$$s_m(t) = \text{Re}\left\{\sum_{n=1}^{N} a_n \exp(j2\pi f_n t + j\phi_n)\right\} \tag{4}$$

where a_n, f_n, ϕ_n are the amplitude, frequency and phase of each tone for $f_j = f_1 + (j-1)\Delta f$, $j = 1, ..., Q$. We assume the minimum tone spacing $\Delta f = T_m^{-1}$ for the symbol time T_m. The maximum transmit PAPR for information transmission can be achieved with uniform power allocation and all initial phases are aligned, $a_n = \sqrt{2P_T/N}$ and $\phi_n = \phi$ for $\forall n$.

To achieve the higher transfer efficiency, we assume that the transmitter performs the precoding for amplitude matching and phase alignment at the receiver with acquired CSI. After the precoding that leads to the maximal-ratio transmission (MRT), the transmitted signal can be expressed as

$$s(t) = \begin{cases} A\frac{h^*}{|h|}\cos(2\pi f_c t + \theta) & \text{for } s_s(t), \\ \sqrt{\frac{2P_T}{N}}\frac{h^*}{|h|}\sum_{n=1}^{N}\cos(2\pi f_n t) & \text{for } s_m(t) \end{cases} \tag{5}$$

where h^* is the conjugate of complex channel gain.

C. Receiver Architecture

As shown in Fig. 1(b), a new receiver architecture is comprised of three (energy/information/PAPR) paths and adaptive PM-&-ID module. To enable the receiver to harvest energy and decode information from the same signal, the power splitter in front of the three paths splits the received signal with power ratio ρ, where $0 < \rho \leq 1$. We assume that infinitesimally small ρ is enough to achieve a proper SNR for information decoding because of the property of integrated receiver [4]. Then, most of the signal power can be harvested at the EH circuit. After power splitting, the received signal at energy path can be expressed as

$$y_{EH}(t) = \sqrt{1-\rho}hs(t) + n(t) \tag{6}$$

where $n(t)$ is the channel noise modeled as $n(t) \sim \mathcal{CN}(0, \sigma^2)$. The resulting DC power P_{EH} is evaluated as

$$P_{EH} = \hat{\Psi}_{EH}(P_R) \times P_R \tag{7}$$

where $P_R = \mathbb{E}[|y_{EH}(t)|^2] = (1-\rho)|h|^2 P_T$ (energy harvested from the noise is ignored), which can be used for charging battery and information decoding at information path as well (see Fig. 1(b)). Note that the signal power of energy path is sufficient enough to ignore the noise power due to small ρ. This implies that the energy-level information from *energy path* can be decoded in almost noise-free condition (high SNR), which assures the performance gain compared to conventional SWIPT that decodes both amplitude and phase information in relatively low SNR.

The received signal for information decoding is of the form

$$y_{ID}(t) = \sqrt{\rho}hs(t) + n(t). \tag{8}$$

Information path is used to decode the phase information of the received signal that is mapped to a constellation point for a given energy level. Because amplitude and phase are very sensitive to channel fading, we assume that channel estimation is performed before decoding, which requires more circuit power consumption relative to that of PAPR based SWIPT. The phase can be measured through conventional PSK phase estimator (e.g., correlator), or low-power circuit whose design is omitted due to space limitation. The phase information can be decoded once the energy level of signal constellation is acquired. Thus, both energy and information paths are jointly combined for the proposed single tone SWIPT.

PAPR path is used for PAPR based information decoding. Since the information is mapped to distinct levels of PAPR, PAPR estimator simply measures the PAPR of the received signal envelope. The received PAPR in FF channel can be evaluated as

$$PAPR = \frac{\max_{t\in[0,T_m]}|y_{ID}(t)|^2}{\frac{1}{T_m}\int_{T_m}|y_{ID}(t)|^2 dt} \cong 2N. \tag{9}$$

It requires less power compared to information path because PAPR based modulation does not require the power-hungry active devices, such as mixer and ADC, as well as channel estimation. Further, the efficiency of WPT in low power region

is enhanced thanks to multi-sine waveforms. Thus, PAPR path is suitable for keeping low circuit power consumption with increased operational range, but offering lower rate.

Adaptive PM-&-ID module monitors the received power and controls the communication mode according to adaptive PM-&-ID policy, which will be addressed in next section. For instance, when the received power changes high to low, the module feedbacks the control message to the transmitter for changing the communication mode and activates PAPR path. Otherwise, it activates information path.

III. Adaptive Mode Switching Policy

In conventional SWIPT, we see discrimination in achievable rate depending on the distance from AP. But with the proposed dual mode operation for SWIPT, the rate discrimination can be mitigated well, leading to increased operational range. The achievable rate of single/multi-tone mode is evaluated as

$$R_s = (1 - p_{out}(M)) \log_2 M, \tag{10}$$

$$R_m = \frac{1}{BT_m}(1 - p_{out}(Q)) \log_2 Q \tag{11}$$

for the signal bandwidth B. The roll-off factor of the single tone mode is set to zero for the minimum Nyquist bandwidth (i.e., symbol time $T_s = B^{-1}$). The outage probability can be defined as $p_{out} = \Pr[p_b > p_{tag}]$, i.e., the bit error rate (BER) given M or Q is higher than the target BER. We assume that $p_{tag,s}$ for single tone mode is tighter than $p_{tag,m}$ for multi-tone mode because the former is optimized for high data rate. In this paper, the above statistical parameters were obtained by Monte Carlo simulations. Also, the circuit power consumption should not exceed the harvested power to ensure the energy causality at the receiver. Note that the energy constraint of each mode is different because the former requires more complex decoding procedure (i.e., channel estimation and I/Q down conversion) than the latter with PAPR based modulation.

We can formulate an adaptive mode switching optimization problem which chooses a proper mode with modulation index M and multi-tone Q, so as to maximize the achievable rate, depending on the received power threshold P_{th} obtained from the non-linear EH model and QoS constraints given above. With $P_R \geq P_{th}$, the optimization for single tone mode (P1) can be formulated as

$$\begin{aligned} \text{(P1)}: \max_{M} \quad & R_s \\ \text{s.t.} \quad & P_{EH} \geq P_{C,s} \\ & p_b(M) \leq p_{tag,s}, \end{aligned}$$

where $P_{C,s}$ is the circuit power consumption of the single tone mode. Otherwise, the optimization for multi-tone mode (P2) with $P_R < P_{th}$ is formulated as

$$\begin{aligned} \text{(P2)}: \max_{Q} \quad & R_m \\ \text{s.t.} \quad & P_{EH} \geq P_{C,m} \\ & p_b(Q) \leq p_{tag,m} \end{aligned}$$

where $P_{C,m}$ is the multi-tone mode circuit power consumption. We can obtain the optimal solution (M^*, Q^*) numerically by running the algorithm described below.

Algorithm 1 Algorithm for adaptive PM-&-ID policy

```
Initialize the maximum number of moduation sub-index i_max and calculate P_EH from P_R
if P_R ≥ P_th and P_EH ≥ P_{C,s} then
    Set modulation sub-index to i = 1
    repeat
        if p_b(2^i) ≤ p_{tag,s} then
            i = i + 1
        else
            return M* = 2^{i-1}, and R_s
        end if
    until constraint of (P1) is satisfied
else if P_R < P_th and P_EH ≥ P_{C,m} then
    Set modulation sub-index to i = i_max
    repeat
        if p_b(2^i) > p_{tag,m} then
            i = i - 1
        else
            return Q* = 2^i, and R_m
        end if
    until constraint of (P2) is satisfied
else
    Set M* = 1 and Q* = 1
end if
```

Note that if the optimal solution M^* or Q^* is less than 2, the information cannot be sent or decoded properly, which implies that the transceiver operates for energy harvesting only.

IV. Numerical Results

In this section, the performance of the proposed dual mode SWIPT and conventional SWIPT schemes is compared. We assume $B = 1$MHz bandwidth where the center frequency f_c is 900MHz. We consider Rayleigh FF channel, and the path-loss exponent is set to 2.5. Also, the noise power is assumed to be -130dBm/Hz. The power-splitting ratio ρ is set to 10^{-6}. For smoothing spline curve fitting of the proposed non-linear EH model, we set $\lambda = 0.06235$. We assume that the transmit power is $P_T = 40$dBm.

Fig. 3 shows the BER performance of the proposed single/multi-tone mode SWIPT receiver when $M = 2, 4, 8$ and $Q = 2, 4$. The performance of conventional 8-QAM SWIPT receiver is also plotted for comparison. The results show that the proposed single tone mode gives better BER performance than conventional SWIPT for the same modulation index $M = 8$. This is because the proposed single tone mode jointly decodes the energy level and its associated phase information, where the energy-level information is less sensitive to noise compared to the existing scheme. Also, the single tone mode shows better performance than the multi-tone mode because of channel estimation at information path. Based on the BER performance, the outage probability versus distance from AP is plotted in Fig. 4. In previous section, we have assumed that the single tone mode needs strict BER constraint to support high data rate. Thus, the target BER of each mode here is set

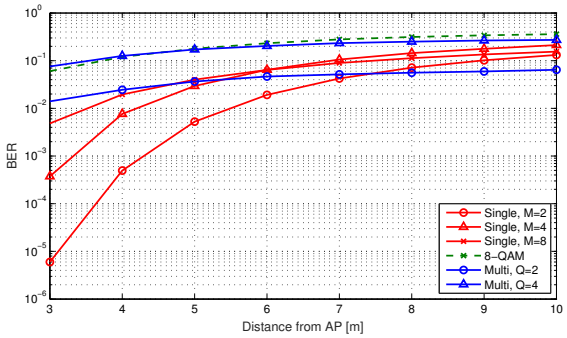

Fig. 3. Bit error rate (BER) versus distance from AP when $P_T = 40$dBm.

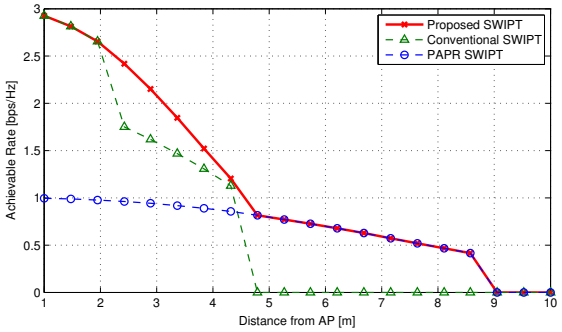

Fig. 5. Achievable rate distribution subject to the QoS constraints.

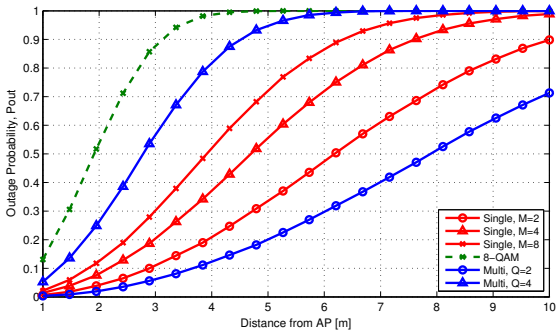

Fig. 4. Outage probability p_{out} versus distance from AP, assuming $p_{tag,s} = 0.01$ and $p_{tag,m} = 0.05$.

to $p_{tag,s} = 0.01$ and $p_{tag,m} = 0.05$, accordingly. We observe that there is a performance gap between the proposed SWIPT and existing QAM based SWIPT schemes.

In Fig. 5, the achievable rate versus distance from AP is depicted, subject to the QoS constraints. We set $P_{th} = 0.5$mW, and the energy causality constraint is set to be $P_{C,s} = 0.2$mW and $P_{C,m} = 0.01$mW. The performance is obtained by taking the average over different channel realizations. Compared to conventional SWIPT, the proposed dual mode SWIPT increases the operational range thanks to the dual mode operation, where MS is occurred around 5m for a given P_{th}. It can be observed that the proposed dual mode SWIPT provides not only increased operational range than conventional QAM based SWIPT, but also yields better achievable rate than PAPR based SWIPT when the receiver is close to the transmitter. This is because the adaptive PM-&-ID policy switches mode and chooses optimum M and Q according to the received power for maximizing the achievable rate.

V. Conclusion

In this paper, we have proposed a novel dual mode SWIPT transceiver architecture with single and multi-tone waveform design. We also suggested a new concept of adaptive power management and information decoding policy based on the proposed smoothing spline curve fitting non-linear EH model. The proposed SWIPT system mitigates the energy causality problem of IoT devices and extends the operational range via the dual mode operation. Performance evaluation demonstrated that the proposed dual mode SWIPT provides significant gain in achievable rate distribution over the existing SWIPT scheme. Especially, the mode switching policy combined with dual mode SWIPT transceiver was shown to be a promising technique for enlarging the operational range of self-sustainable green communication.

Future study will look into the mathematical system optimization of the proposed transceiver and adaptive PM-&-ID policy to adjust key system parameters, such as the received power threshold P_{th}. Further, we will implement a dual mode SWIPT prototype on real RF circuit and perform experimentation under various network and channel conditions.

Acknowledgment

This work was supported by the National Research Foundation of Korea (NRF) grant funded by the Korean government (MSIP) (2014R1A5A1011478).

References

[1] X. Lu, P. Wang, D. Niyato, D. I. Kim, and Z. Han, "Wireless networks with RF energy harvesting: A contemporary survey," *IEEE Commun. Surveys & Tutorials*, vol. 17, no. 2, pp. 757-789, Second Quarter 2015.

[2] X. Lu, P. Wang, D. Niyato, D. I. Kim, and Z. Han, "Wireless charging technologies: Fundamentals, standards, and network applications," *IEEE Commun. Surveys & Tutorials*, vol. 18, no. 2, pp. 1413-1452, Second Quarter 2016.

[3] Y. Zeng, B. Clerckx, and R. Zhang, "Communications and signals design for wireless power transmission," *IEEE Trans. Commun.*, vol. 65, no.5, pp. 2264-2290, Mar. 2017.

[4] X. Zhou, R. Zhang, and C. K. Ho, "Wireless information and power transfer: Architecture design and rate-energy tradeoff," *IEEE Trans. Commun.*, vol. 61, no.11, pp. 4754–4767, Nov. 2013.

[5] E. Boshkovska, D. W. K. Ng, N. Zlatanov, and R. Schober, "Practical non-linear energy harvesting model and resource allocation for SWIPT systems," *IEEE Commun. Letters*, vol. 19, no. 12, pp. 2082-2085, Dec. 2015.

[6] A. Boaventura, D. Belo, R. Fernandes, A. Collado, A. Georgiadis, and N. B. Carvalho, "Boosting the efficiency: Unconventional waveform design for efficient wireless power transfer," *IEEE Microw. Mag.*, vol. 16, no. 3, pp. 87-96, Apr. 2015.

[7] B. Clerckx, and E. Bayguzina, "Waveform design for wireless power transfer," *IEEE Trans. Signal Processing*, vol. 64, no. 23, pp. 6313-6328, Dec. 2016.

[8] M. R. V. Moghadam, Y. Zeng and R. Zhang, "Waveform optimization for radio-frequency wireless power transfer," arXiv: 1703.04006

[9] D. I. Kim, J. H. Moon, and J. J. Park, "New SWIPT using PAPR: How it works," *IEEE Wireless Commun. Letters*, vol. 5, no. 6, pp. 672-675, Dec. 2016.